



## Integration of cortical thickness data in a statistical shape model of the scapula

Jonathan Pitocchi<sup>a,b,c</sup> , Roel Wirix-Speetjens<sup>a</sup>, G. Harry van Lenthe<sup>c</sup>  and María Ángeles Pérez<sup>b</sup>

<sup>a</sup>Materialise NV, Heverlee, Belgium; <sup>b</sup>Multiscale in Mechanical and Biological Engineering (M2BE), University of Zaragoza, Zaragoza, Spain; <sup>c</sup>Biomechanics Section, KU Leuven (University of Leuven), Leuven, Belgium

### ABSTRACT

Knowledge about bone morphology and bone quality of the scapula throughout the population is fundamental in the design of shoulder implants. In particular, regions with the best bone stock (cortical bone) are taken into account when planning the supporting screws, aiming for an optimal fixation. As an alternative to manual measurements, statistical shape models (SSMs) have been commonly used to describe shape variability within a population. However, explicitly including cortical thickness information in an SSM of the scapula still remains a challenge. Therefore, the goal of this study is to combine scapular bone shape and cortex morphology in an SSM. First, a method to estimate cortical thickness, based on HU (Hounsfield Unit) profile analysis, was developed and validated. Then, based on the manual segmentations of 32 healthy scapulae, a statistical shape model including cortical information was created and evaluated. Generalization, specificity and compactness were calculated in order to assess the quality of the SSM. The average cortical thickness of the SSM was  $2.0 \pm 0.63$  mm. Generalization, specificity and compactness performances confirmed that the combined SSM was able to capture the bone quality changes in the population. In this work we integrated information on the cortical thickness in an SSM for the scapula. From the results we conclude that this methodology is a valuable tool for automatically generating a large population of scapulae and deducing statistics on the cortex. Hence, this SSM can be useful to automate implant design and screw placement in shoulder arthroplasty.

### ARTICLE HISTORY

Received 16 September 2019  
Accepted 14 April 2020

### KEYWORDS

Statistical shape model;  
reverse shoulder  
arthroplasty; cortical  
thickness; scapula;  
population analysis;  
implant design

## Introduction

Statistical shape models (SSMs) provide a valuable way to describe shape variability within a training dataset. Since their introduction (Cootes and Taylor 2001), these models have been used for multiple applications: to automatically segment bone structures (Lamecker et al. 2004; Ma et al. 2017), to study the shapes of human anatomy (Sarkalkan et al. 2014; Salhi et al. 2017; Sintini et al. 2018; Casier et al. 2018), to virtually reconstruct large bone defects (Vanden Berghe et al. 2017; Poltaretskyi et al. 2017; Plessers et al. 2018; Abler et al. 2018), to build 3D models starting from 2D information (Grassi et al. 2017; Mutsvangwa et al. 2017). The main concept behind SSM techniques is to perform principal component analysis (PCA) on corresponding landmarks derived from the dataset objects and to extract the main modes of variation. Thus, each subject in the training dataset can be described by a linear combination of principal components (PCs), corresponding

to these modes of variation. Moreover, new instances, representative of the population, can be generated by varying the PC (Cootes and Taylor 2001).

In addition to quantifying shape variation, SSMs may be combined with bone quality information (such as image intensities, cortical thickness, etc.) in order to create combined models. Such information can be used in population studies to explore cortical variation in the main region of interest for implant and screw placement. This way, guidelines that function for the overall population, can be defined for the design of robust implant and the positioning of the screws (DiStefano et al. 2011).

In a previously published study (Bonaretti et al. 2014), a statistical appearance model of the femur, combining both shape and image intensities variation, was created using two workflows (an image-based and a mesh-based approach) to generate ready-to-run finite element model that can be used in the in silico assessment of bone quality and strength. In a recent

**CONTACT** Jonathan Pitocchi  [jonathan.pitocchi@materialise.be](mailto:jonathan.pitocchi@materialise.be)

© 2020 Informa UK Limited, trading as Taylor & Francis Group

This is an Open Access article distributed under the terms of the Creative Commons Attribution-NonCommercial-NoDerivatives License (<http://creativecommons.org/licenses/by-nc-nd/4.0/>), which permits non-commercial re-use, distribution, and reproduction in any medium, provided the original work is properly cited, and is not altered, transformed, or built upon in any way.

work (Zhang et al. 2016), it was demonstrated, on a large population of femur, that cortical information can be integrated to create statistical models with cortical thickness. In their study, cortical bone mapping (Treece et al. 2010) was used to automatically detect cortical thickness over the entire femoral surface.

Few studies have tried to create a combined model for the scapula. Burton et al. (2019) developed an SSM and a statistical intensity model (SIM) to explore the variation in shape and material property distribution throughout the population. In their study, volumetric meshes were created to include the bone quality information in the statistical shape model. Only the layer of elements in the surface (size  $1.0 \pm 0.2$  mm) was used to represent the cortical bone, thus their approach was limited in describing the variation in cortical thickness within and between subjects.

In order to explicitly include subject specific cortical thickness information on the SSM, additional efforts must be done. The scapula morphology is complex and the trabecular region is not one continuous region. For other anatomies (e.g., femur), where often a clear trabecular structure is present, it is possible to use standard SSM workflows (where point correspondence between outer and inner surface is obtained by warping). For the scapula this is not a viable option, but the sparse trabecular information can be included in the model through cortical scalar values. Therefore, the goal of this study is to combine scapular bone shape and cortex morphology in an SSM. First, an automatic method to estimate cortical thickness, based on HU-profile analysis, is developed and validated, as an alternative to the one used in (Treece et al. 2010). Second, a technique is presented to include cortical thickness in the SSM of the scapula. The quality of the created SSM is then evaluated by assessing the generalization, the specificity and the compactness of the resulting model.

## Materials and methods

### Dataset

A set of 32 scapulae, 17 males and 15 females, was selected by an experienced surgeon for the construction and evaluation of the SSM. All computed tomography scans were visually inspected and only scapulae without glenohumeral arthropathy signs were included. The average age was  $59 \pm 12$  years. The youngest patient was 28 years old and the oldest 74. The dataset was already used in Plessers et al. (2018) for the creation of an SSM to virtually reconstruct glenoid bone defects. The scapula scans were segmented in the image processing software Mimics v.20

(Materialise, Leuven, Belgium) and converted to three-dimensional models, with a mean triangular edge length of 1.5 mm. The 3D models were obtained using the approach described in a previous work (Van den Broeck et al. 2014). In the study, a segmentation workflow for the construction of three-dimensional models from clinical CT-scans, was validated for medical applications.

### Cortical thickness estimation

An algorithm was developed in Python 3.5 to automatically estimate sampled cortical thickness (Figure 1) starting from the initial three-dimensional model. For each point in the model surface, HU values were sampled along the line passing through that point and perpendicular to the surface, with a sampled distance of 0.1 mm. As a result, a HU profile was obtained for each point in the surface. First, a threshold of 226 HU was applied to detect the cortical bone in the profile and separate cortical and trabecular values. The full-width at half maximum method (FWHM) was used to estimate the cortical thickness by setting the 10th percentile of the trabecular intensities as the value for the trabecular bone. Using a Variable Wrapped Offset algorithm, it was possible to build the inner surface (representing the trabecular bone) by setting the measured cortical thickness as local offset for each point of the outer surface. The algorithm makes use of a `vtkContourFilter` to generate the Isosurface mesh from the scalar values (VTK: `vtkContourFilter` Class Reference).

### Validation of cortical thickness estimation

The cortical thickness algorithm was evaluated by comparing its results with manually segmented cortex, for a random subset of 10 scapulae. First, starting from the surface obtained through the automatic algorithm, a mask on the original CT-image was extracted. Then, to take into account for inter-operator variability, three operators were asked to manually segment the same dataset of scapulae. Using the ITK implementation of the STAPLE algorithm (Warfield et al. 2002), the ground truth was generated from the three expert segmentations for each case. The STAPLE algorithm treats segmentation as a pixel-wise classification, which leads to an averaging scheme that accounts for systematic biases in the behaviour of experts in order to generate a ground truth volume and a simultaneous accuracy assessment of each expert. Thus, accuracy parameters (sensitivity, specificity and dice coefficient, DC) could be

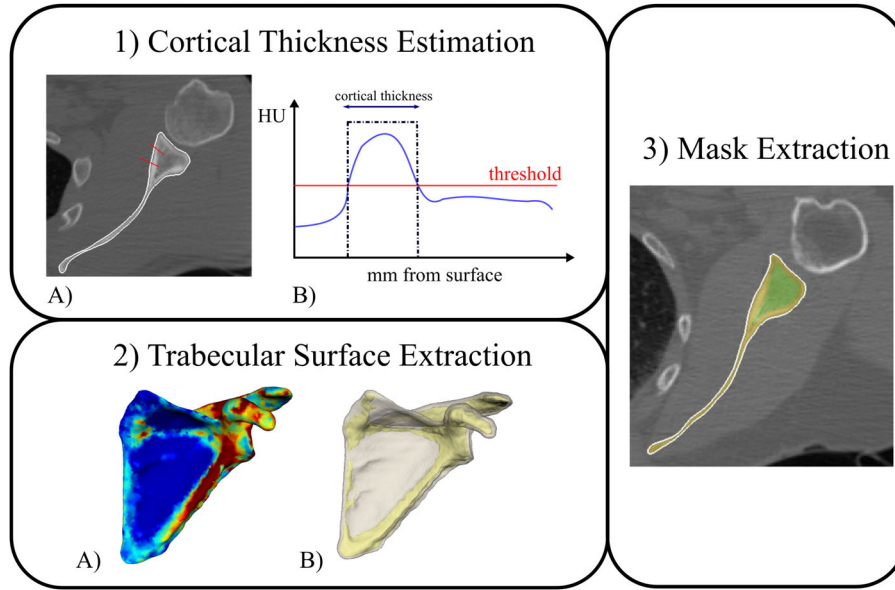


**Figure 1.** The subsequent steps in the estimation of the cortical thickness: cortical thickness is estimated for each surface point (1A) by sampling HU values along lines perpendicular to the surface and using a threshold-based method (1B). The cortical values (2A) are set as local offset of a Variable Wrapped Offset algorithm to build the trabecular surface (2B). Finally, from the surface a mask is extracted on the image for comparison against manual segmentation (3).

extracted for each operator by comparing the golden truth obtained with the STAPLE algorithm to the original manual segmentation. Then the accuracy of the automatic algorithm was evaluated against the golden truth and the performance was compared to that of the manual segmentation (mean  $\pm$  standard deviation of the three operators).

### SSM construction

An SSM was created in three subsequent steps, as presented in Vanden Berghe et al. (2017). First, one model of the dataset was registered to all other models to obtain corresponding surfaces. Second, the models were aligned to exclude all translational and rotational variations. No scaling was performed to maintain the size information of the models. Similarly to a previously described approach (Zhang et al. 2016), the cortical thickness value of each surface point was directly integrated in the data matrix to produce a model of shape variation correlated with cortical thickness variations. In this way, each column  $X_i$  of the data matrix contained the concatenated point coordinates of the training dataset and the corresponding cortical thickness values (Cootes and Taylor 2001):

$$X_i = \{x_{i,1}, x_{i,2}, \dots, x_{i,n}, y_{i,1}, y_{i,2}, \dots, y_{i,n}, z_{i,1}, z_{i,2}, \dots, z_{i,n}, s_{i,1}, s_{i,2}, \dots, s_{i,n}\}^T, \quad (1)$$

where  $x_i$ ,  $y_i$ ,  $z_i$  are the three-dimensional coordinates of node  $i$  and  $s_i$  are the corresponding cortical

thickness values. Finally, PCA was applied to the data matrix.

### SSM evaluation

To assure the construction of a high quality SSM, we applied different tests (Davies and Taylor 2008). A visual inspection of the SSM modes of variation was done to ensure that no unnatural shape and cortical variation were present in the model. Compactness was evaluated in order to assess how efficiently the variation in the dataset can be represented by the model. Two fundamental properties that are commonly used to assess the good quality of a model, were measured: specificity and generalization ability.

The specificity ability can be used to quantify how much new cases generated through the SSM differ from the cases included in the training set. It is implied that a good SSM should generate only models representative of the described anatomy. Specificity was evaluated by sampling new instances with a certain number of modes, and comparing them to the most similar cases of the training set.

The generalization ability of an SSM measures how well new data samples can be represented by the model for a certain number of modes of variation. Generalization was evaluated by performing a Leave-One-Out (LOO) test. To evaluate the ability of the model to generalize the cortical information, the trabecular surface was reconstructed and the Euclidean

**Table 1.** Accuracy results of the cortical segmentation for a random subset of 10 scapulae. For the inter-operator, mean  $\pm$  standard deviation was obtained by evaluating the segmentation of three operators against the golden truth generated with the STAPLE algorithm. The accuracy of the automatic algorithm was evaluated against the same golden truth.

		Case 1	Case 2	Case 3	Case 4	Case 5	Case 6	Case 7	Case 8	Case 9	Case 10	Mean	Std
Inter-operator	Sensitivity	93.9 $\pm$ 6.3	95.7 $\pm$ 4.4	96.0 $\pm$ 2.9	94.8 $\pm$ 3.9	95.6 $\pm$ 5.0	96.0 $\pm$ 3.1	94.3 $\pm$ 5.1	95.5 $\pm$ 2.8	95.5 $\pm$ 4.5	94.5 $\pm$ 4.7	95.4	4.4
	Specificity	99.0 $\pm$ 0.9	93.4 $\pm$ 8.1	93.3 $\pm$ 8.3	96.3 $\pm$ 2.1	97.9 $\pm$ 0.7	97.6 $\pm$ 1.4	98.7 $\pm$ 0.7	85.5 $\pm$ 20.4	92.5 $\pm$ 6.8	97.8 $\pm$ 0.9	94.9	8.8
	Dice Coefficient	96.6 $\pm$ 3.5	96.3 $\pm$ 2.3	96.7 $\pm$ 2.2	96.7 $\pm$ 1.94	97.3 $\pm$ 2.5	97.3 $\pm$ 2.0	96.7 $\pm$ 2.8	95.7 $\pm$ 3.3	96.3 $\pm$ 1.8	96.7 $\pm$ 2.6	96.7	2.5
Automatic Algorithm	Sensitivity	94.3	95.8	94.5	94.8	93.8	93.7	93.4	94.4	91.9	91.6	93.8	1.2
	Specificity	90.3	87.5	89.1	87.1	92.7	87.7	87.1	87.0	86.8	90.2	88.6	1.9
	Dice Coefficient	95.7	95.1	95.2	95.2	95.7	93.8	94.0	94.8	93.5	94.1	94.7	0.8

distance between the original trabecular surface and the reconstructed one was calculated. Finally, we evaluated the generalization of the model on an image level. We extracted a mask from the two trabecular surfaces (the test case and the reconstructed one) and for this we evaluated the accuracy of the generalization by calculating the Dice score.

## Results

### Cortical thickness estimation

The results of the inter-operator analysis and the accuracy of the automatic algorithm are presented in Table 1. For each case, the mean and the standard deviation of the performances of the three operator is reported for sensitivity, specificity and Dice score. In the last column, the mean and the standard deviation is reported for all the dataset, both for manual and automatic segmentation. All the accuracy parameters of the manual segmentation show a higher standard deviation when compared to that of the automatic algorithm. The performances of the automatic algorithm remain inside the inter-operator variability: 93.8  $\pm$  1.2 versus 95.4  $\pm$  4.4 for the sensitivity, 88.6  $\pm$  1.9 versus 94.9  $\pm$  8.8 for the specificity and 94.7  $\pm$  0.8 versus 96.7  $\pm$  2.5 for the Dice coefficient.

### SSM analysis

The average cortical thickness of the SSM was 2.0  $\pm$  0.6 mm. The shape and the cortical thickness variation in the first two modes of variation are represented in Figure 2. The first mode mainly models the scaling variation of the model set. When considering a large scapula ( $-2\sigma$ ), greater thickness values are expected, whereas while considering a small scapula, lower thickness values are observed. The second mode shows a variation in the glenoid inclination and acromion orientation, with no visible relation to the cortical thickness variation.

The first mode of variation explained 77% of all data variation and the SSM explained more than 95% of all data variation with 12 modes (Figure 3(A)). The results

of the generalization for the outer surface are represented in Figure 3(B). At the first mode, the median error for the outer surface was about 3 mm while it reached a plateau in performance around 1.5 mm.

A random sample of 1000 new instances was generated to measure the specificity both for the outer surface and the cortical thickness values (Figure 4). For the outer surface, the specificity started to converge after 25 modes, reaching a root-mean-square-error (RMSE) of 3.1  $\pm$  0.54 mm when using all 32 modes to generate the new cases (Figure 4(A)). For the cortical values, although fully convergence was not reached, a RMSE of 0.67  $\pm$  0.12 mm was measured with 32 modes (Figure 4(B)).

Figure 5 shows instead the results of the generalization for the trabecular surface. The median error decreased from 3 mm at the first mode to 1.5 mm for the plateau zone. The Dice coefficient, calculated as the overlap between the mask of the original trabecular surface and the reconstructed one, increased from a value of almost 0.6 at the first mode, to a value slightly below 0.8.

## Discussion

The main objective of this study was to provide a statistical description of the morphology and cortical bone thickness of the scapula by using statistical shape modelling techniques. It is well established that cortical bone distribution plays a fundamental role in the assessment of the fixation of shoulder implants, in particular for screw placement and orientation (Codsi et al. 2007; Daalder et al. 2018). In the current study, an automatic algorithm for cortical thickness estimation was developed and validated against manual segmentations. The inter-operator study demonstrated a high variability of the output (Table 1). This result underlines that the segmentation of cortical bone in the scapula remains a difficult task also for expert operators. The automatic algorithm shows results comparable to the inter-operator variability, thus addressing the validity of the algorithm. Thicker cortical regions were present in the scapular notch and spine, lateral border of

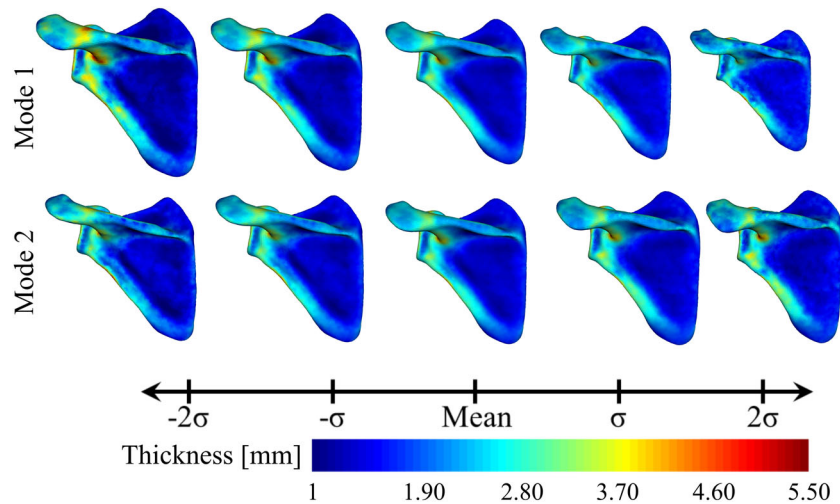


**Figure 2.** Shape and cortical thickness variation in the first two modes of variations. For mode 1 (top), when passing from a large scapula ( $-2\sigma$ ) to a small scapula ( $+2\sigma$ ), a decrease in cortical thickness is visible. Mode 2 (bottom) shows a variation in the glenoid inclination and acromion orientation, with no visible relation to the cortical values.

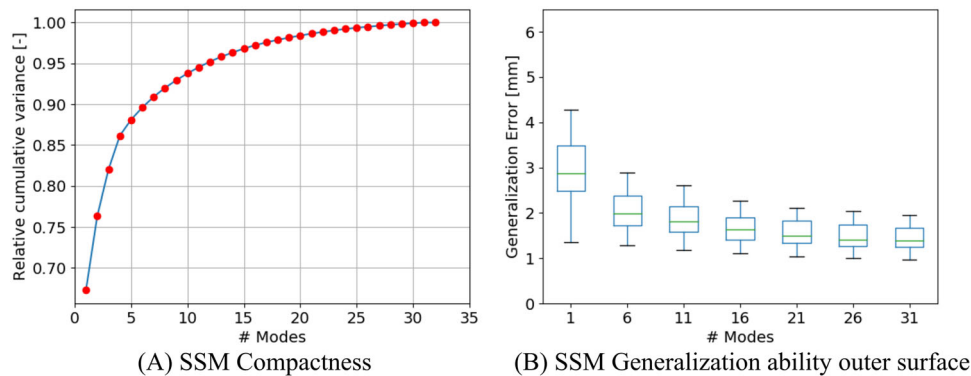


**Figure 3.** Analysis of the SSM quality. (A) Compactness of the SSM. (B) Generalization ability for the shape variation of the outer surface.

the scapula and junction of glenoid neck, similarly to DiStefano et al. (2011). The presented method was able to describe the subject-specific variation of cortical bone and provide meaningful information to include in the SSM. In future, other techniques may be investigated and integrated in the current workflow, such as cortical bone mapping (CBM) (Treece et al. 2010). In particular, our approach did not consider the impact of the CT-resolutions on the cortical estimation. On the contrary, CBM have proven to be able to estimate very thin cortices that are well within the resolution of the CT scanner through optimization methods. Its application to the scapula morphology would have required validation against high-quality images, which was not available for the presented dataset.

Furthermore, a workflow was presented and validated to include bone quality information in an SSM and subsequently applied to a training dataset of 32 patients. The compactness and generalization error for the outer surface (1.5 mm) is comparable to the

one of similar studies (Burton et al. 2019). The specificity analysis results in a good convergence for the outer surface RMSE, while fully convergence could not be reached for the cortical values, possibly due to the limited number of training cases.

When looking to the generalization ability for the trabecular surface, both the Euclidean distance and the Dice score show good performances of the combined SSM. In general, the results demonstrate a high variability of the cortical distribution throughout the population, suggesting that any implant must be designed to accommodate the variation in bone quality. In a clinically relevant application, shoulder standard implants could be virtually implanted in the mean shape of the model to check for congruency between the screws position and the distribution of cortical thickness. Similarly, through a population study, the cortical thickness distribution could be assessed for different subgroups of the population (based on gender, sex, age) thus allowing for designs that best fit a specific subgroup.

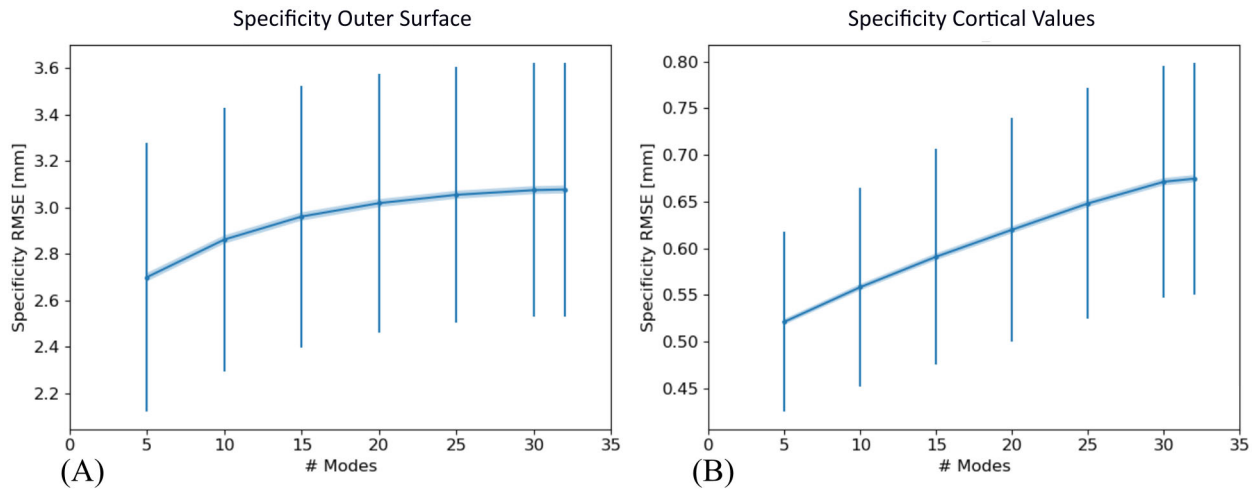


**Figure 4.** Specificity ability of the SSM evaluated for the outer surface (A) and the cortical values (B). A random sample of 1000 new instances was generated to measure the specificity.

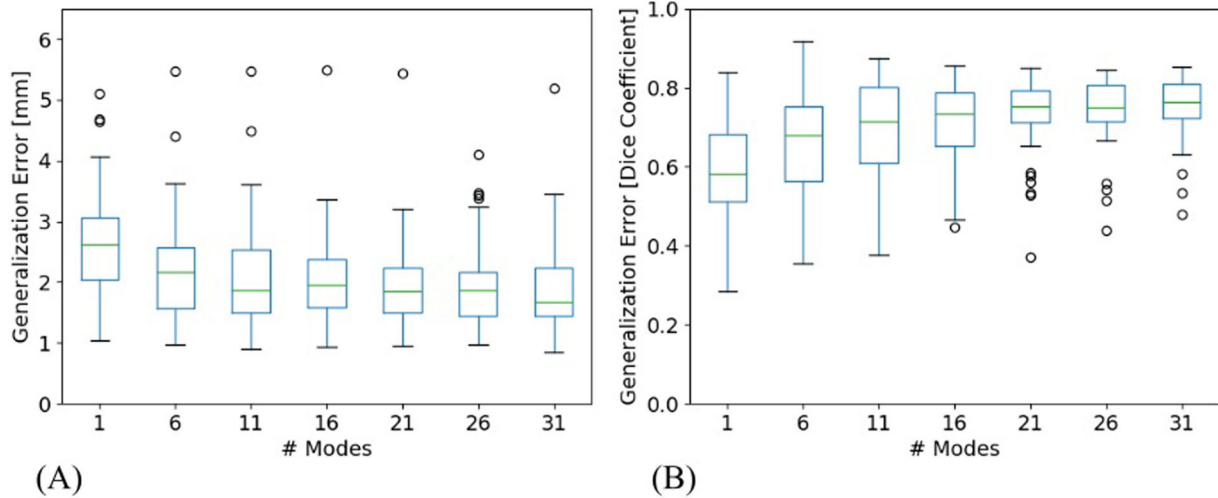


**Figure 5.** Distance (A) and Dice score (B) performances for the generalization of the trabecular surface. The distance error represents the RMSE of the Euclidean distance between the original and the reconstructed trabecular surfaces. The Dice score is calculated on the masks extracted from the two trabecular surfaces (original and reconstructed).

Some limitations to this study need to be acknowledged. During the construction of the SSM, cortical thickness values and point coordinates were concatenated without any normalization to build the data matrix, following the approach described in Zhang et al. (2016). Hence, the difference in scales could bias the model. Although a thorough evaluation of the SSM was performed, further analysis is necessary to evaluate the possible impact of the bias on our analysis.

The modes of variation captured in the statistical models are strongly dependent on the training dataset. One of the main limitations of this study is the number of training subjects. A dataset of 32 scapulae may probably be not enough to fully represent the global population. Moreover, the workflow was applied to a dataset of healthy scapulae. However, the study was primarily focus

on describing an automatic method to integrate cortical thickness information in an SSM of the scapula. Future work may include the extension of the dataset as well as the application to non-healthy populations that are of interest from a shoulder replacement perspective.

## Conclusions

In this work we integrated for the first time, to our knowledge, information on the cortical thickness in an SSM for the scapula. The results demonstrate that this methodology is a valuable tool for automatically generating a large population of scapulae and deducing statistics on the cortex. Moreover, based on this pipeline, a statistical FE model, including an explicit model of the cortical bone, could be automatically

created to perform statistical analysis of biomechanical performance across a given population.

## Disclosure statement

No potential conflict of interest was reported by the authors.

## Funding

This work was supported by the Marie Skłodowska-Curie actions (Grant no: 722535).

## ORCID

Jonathan Pitocchi  <http://orcid.org/0000-0002-9165-3888>

G. Harry van Lenthe  <http://orcid.org/0000-0001-8303-4959>

## References

- Abler D, Berger S, Terrier A, Becce F, Farron A, Büchler P. 2018. A statistical shape model to predict the premorbid glenoid cavity. *J Shoulder Elbow Surg.* 27(10):1800–1808.
- Bonaretti S, Seiler C, Boichon C, Reyes M, Büchler P. 2014. Image-based vs. mesh-based statistical appearance models of the human femur: Implications for finite element simulations. *Med Eng Phys.* 36(12):1626–1635.
- Burton WS, Sintini I, Chavarria JM, Brownhill JR, Laz PJ. 2019. Assessment of scapular morphology and bone quality with statistical models. *Comput Methods Biomech Biomed Eng.* 22(4):341–351.
- Casier SJ, Van den Broecke R, Van Houcke J, Audenaert E, De Wilde LF, Van Tongel A. 2018. Morphologic variations of the scapula in 3-dimensions: a statistical shape model approach. *J Shoulder Elbow Surg.* 27(12):2224–2231.
- Codsi MJ, Bennetts C, Powell K, Iannotti JP. 2007. Locations for screw fixation beyond the glenoid vault for fixation of glenoid implants into the scapula: an anatomic study. *J Shoulder Elbow Surg.* 16(3):S84–S89.
- Cootes TF, Taylor CJ. 2001. Statistical models of appearance for medical image analysis and computer vision. In: *Medical Imaging 2001: Image Processing*. Vol. 4322. International Society for Optics and Photonics; p. 236–248.
- Daalder MA, Venne G, Sharma V, Rainbow M, Bryant T, Bicknell RT. 2018. Trabecular bone density distribution in the scapula relevant to reverse shoulder arthroplasty. *JSES Open Access* 2(3):174–181.
- Davies R, Taylor C. 2008. *Statistical models of shape: optimisation and evaluation*. London: Springer-Verlag.
- DiStefano JG, Park AY, Nguyen T-Q, Diederichs G, Buckley JM, Montgomery WH. 2011. Optimal screw placement for base plate fixation in reverse total shoulder arthroplasty. *J Shoulder Elbow Surg.* 20(3):467–476.
- Grassi L, Väänänen SP, Ristinmaa M, Jurvelin JS, Isaksson H. 2017. Prediction of femoral strength using three-dimensional finite element models reconstructed from DXA images: validation against experiments. *Biomech Model Mechanobiol.* 16(3):989–1000.
- Lamecker H, Seebaß M, Hege H-C, Deuffhard P. 2004. A 3D statistical shape model of the pelvic bone for segmentation. In: *Medical Imaging 2004: Image Processing*. Vol. 5370. International Society for Optics and Photonics; p. 1341–1351.
- Ma J, Wang A, Lin F, Wesarg S, Erdt M. 2017. nonlinear statistical shape modeling for ankle bone segmentation using a novel kernelized robust PCA. In: *Descoteaux M, Maier-Hein L, Franz A, Jannin P, Collins DL, Duchesne S, editors. Medical image computing and computer assisted intervention – MICCAI 2017*. Vol. 10433. Cham: Springer International Publishing. p. 136–143.
- Mutsvangwa T, Wasswa W, Burdin V, Borotikar B, Douglas TS. 2017. Interactive patient-specific three-dimensional approximation of scapula bone shape from two-dimensional X-ray images using landmark-constrained statistical shape model fitting. In: *2017 39th Annual International Conference of the IEEE Engineering in Medicine and Biology Society (EMBC)*. Seogwipo: IEEE. p. 1816–1819.
- Plessers K, Vanden Berghe P, Van Dijck C, Wirix-Speetjens R, Debeer P, Jonkers I, Vander Sloten J. 2018. Virtual reconstruction of glenoid bone defects using a statistical shape model. *J Shoulder Elbow Surg.* 27(1):160–166.
- Poltaretskyi S, Chaoui J, Mayya M, Hamitouche C, Bercik MJ, Boileau P, Walch G. 2017. Prediction of the pre-morbid three-dimensional anatomy of the proximal humerus based on statistical shape modelling. *Bone Joint J.* 99(7):927–933.
- Salhi A, Burdin V, Mutsvangwa T, Sivarasu S, Brochard S, Borotikar B. 2017. Subject-specific shoulder muscle attachment region prediction using statistical shape models: A validity study. In: *2017 39th Annual International Conference of the IEEE Engineering in Medicine and Biology Society (EMBC)*. Seogwipo: IEEE. p. 1640–1643.
- Sarkalkan N, Weinans H, Zadpoor AA. 2014. Statistical shape and appearance models of bones. *Bone* 60:129–140.
- Sintini I, Burton WS, Sade P, Chavarria JM, Laz PJ. 2018. Investigating gender and ethnicity differences in proximal humeral morphology using a statistical shape model: proximal humeral morphology. *J Orthop Res.* 36(11):3043–3052.
- Treece GM, Gee AH, Mayhew PM, Poole K. 2010. High resolution cortical bone thickness measurement from clinical CT data. *Med Image Anal.* 14(3):276–290.
- Vanden Berghe P, Demol J, Gelaude F, Vander Sloten J. 2017. Virtual anatomical reconstruction of large acetabular bone defects using a statistical shape model. *Comput Methods Biomech Biomed Eng.* 20(6):577–586.
- Van den Broeck J, Vereecke E, Wirix-Speetjens R, Vander Sloten J. 2014. Segmentation accuracy of long bones. *Med Eng Phys.* 36(7):949–953.
- VTK: *vtkContourFilter Class Reference*. 2019. [accessed Feb 11]. <https://vtk.org/doc/nightly/html/classvtkContourFilter.html#details>.
- Warfield SK, Zou KH, Wells WM. 2002. Validation of image segmentation and expert quality with an expectation-maximization algorithm. In: *Dohi T, Kikinis R, editors. Medical image computing and computer-assisted intervention-MICCAI*. Berlin: Springer. p. 298–306.
- Zhang J, Hislop-Jambrich J, Besier TF. 2016. Predictive statistical models of baseline variations in 3-D femoral cortex morphology. *Med Eng Phys.* 38(5):450–457.